Photoacoustics 25 (2022) 100325

Contents lists available at ScienceDirect

Photoacoustics

journal homepage: www.elsevier.com/locate/pacs

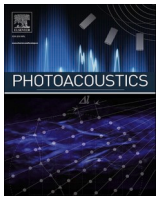

Compact quartz-enhanced photoacoustic sensor for ppb-level ambient NO_2 detection by use of a high-power laser diode and a grooved tuning fork

Shangzhi Li [a,b,1], Juncheng Lu [c,1], Zhijin Shang [a,b], Xiangbao Zeng [d], Yupeng Yuan [d], Hongpeng Wu [a,b], Yufeng Pan [a,b], Angelo Sampaolo [e], Pietro Patimisco [e], Vincenzo Spagnolo [a,e], Lei Dong [a,b,*]

[a] State Key Laboratory of Quantum Optics and Quantum Optics Devices, Institute of Laser Spectroscopy, Shanxi University, Taiyuan 030006, PR China
[b] Collaborative Innovation Center of Extreme Optics, Shanxi University, Taiyuan 030006, PR China
[c] Institute of Information Optics, Zhejiang Normal University, Jinhua 321004, PR China
[d] Chongqing Acoustic-Optic-Electronic Co. Ltd, China Electronics Technology Group, Chongqing 401332, PR China
[e] PolySense Lab-Dipartimento Interateneo di Fisica, University and Politecnico of Bari, Via Amendola 173, Bari, Italy

ARTICLE INFO

Keywords:
Quartz-enhanced photoacoustic spectroscopy
High-power LD module
NO_2 gas sensing
Custom quartz tuning fork

ABSTRACT

A compact quartz-enhanced photoacoustic sensor for ppb-level ambient NO_2 detection is demonstrated, in which a high-power blue laser diode module with a small divergence angle was employed to take advantages of the directly proportional relationship between sensitivity and power, hence improving the detection sensitivity. In order to extend the stability time, a custom grooved quartz tuning fork with 800-μm prong spacing is employed to avoid complex signal balance and/or optical spatial filter components. The sensor performance is optimized and assessed in terms of optical coupling, power, gas flow rate, pressure, signal linearity and stability. A minimum detectable concentration (1σ) of 7.3 ppb with an averaging time of 1 s is achieved, which can be further improved to be 0.31 ppb with an averaging time of 590 s. Continuous measurements covering a five-day period are performed to demonstrate the stability and robustness of the reported NO_2 sensor system.

1. Introduction

Nitrogen dioxide (NO_2) is a red-brown, pungent and toxic gas recognized as a primary air pollutant due to its impact on tropospheric ozone formation and destruction. In addition to natural lightning, ambient NO_2 is mainly released from anthropogenic high-temperature combustion processes, such as vehicle exhaust and boiler exhaust emissions. NO_2 is one of the main causes of photochemical smog and acid rain, thus representing one of the key contributors to the determination of air quality in urban environments [1–5]. Besides that, NO_2 is designated as one of the United States Environmental Protection Agency's (US EPA) "criteria pollutants", therefore the NO_2 concentration is an important indicator in daily urban air pollution index [6,7]. In the atmosphere, the typical average mixing ratio of NO_2 is about 10–30 ppb by volume, but it may even rise by several orders of magnitude in highly polluted areas. Prolonged exposure to NO_2 gas at even low concentration level can lead to respiratory diseases in humans and animals, hence there is a need to develop a robust, sensitive and cost-effective sensor system for atmospheric NO_2 monitoring [8–12].

Various gas analysis techniques have been developed and widely used for NO_2 detection and they are mainly based on the principles of electrochemistry and optics [13–23]. Electrochemical sensors have relatively slow response time, limited lifetime and poor selectivity for NO and NO_2. Compared with electrochemical methods, optical detection techniques for NO_2 measurement can provide the advantages of sensitivity, selectivity, and real-time monitoring, such as differential optical absorption spectroscopy (DOAS) [24], laser-induced fluorescence (LIF) [25], cavity ring-down spectroscopy (CRDS) [26–29] and photoacoustic spectroscopy (PAS) [30,31]. Among them, PAS is one of the most promising techniques to monitor trace gas level due to its benefits of high sensitivity, selectivity, and fast response [32–35]. Besides, PAS-based gas sensors provide two unique interests: (1)

* Corresponding author at: State Key Laboratory of Quantum Optics and Quantum Optics Devices, Institute of Laser Spectroscopy, Shanxi University, Taiyuan 030006, PR China.
E-mail address: donglei@sxu.edu.cn (L. Dong).
[1] These authors contributed equally to this manuscript.

https://doi.org/10.1016/j.pacs.2021.100325
Received 28 October 2021; Received in revised form 30 November 2021; Accepted 15 December 2021
Available online 16 December 2021

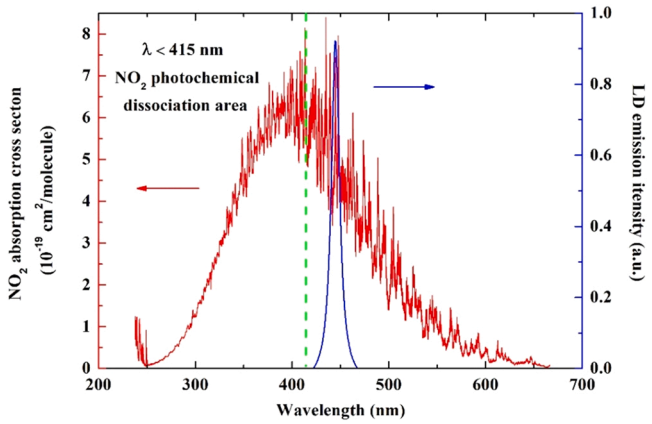

Fig. 1. NO_2 absorption cross section between 250 nm and 650 nm (red) including the photochemical dissociation area with $\lambda < 415$ nm (green) and emission spectrum of the high-power blue LD module (blue).

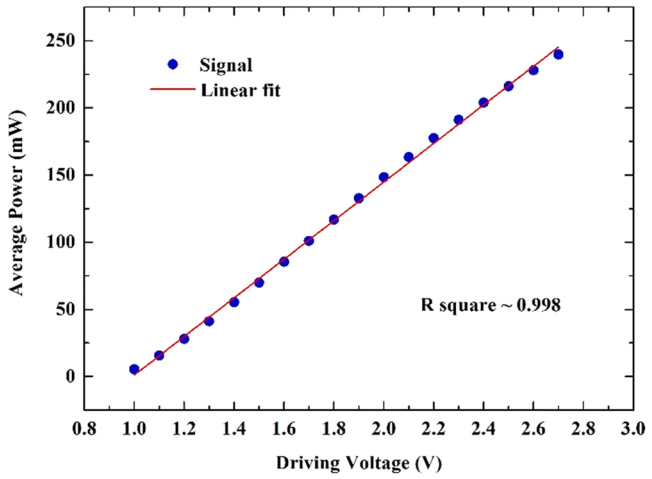

Fig. 2. The average optical power as a function of the LD driving voltage.

Wavelength independence, meaning that trace gas with different characteristic absorption spectrum can be measured by employing the same spectrophone and the photodetector is not required; (2) The directly proportional relationship between sensitivity and incident laser power, which means that use of a higher laser power could provide better sensing performance.

Quartz-enhanced photoacoustic spectroscopy (QEPAS), a modification of the PAS, was first reported and demonstrated in 2002 [36,37]. In QEPAS-based sensors, commercially available piezoelectric quartz tuning fork acoustically couples with two acoustic micro resonators (AmRs) acting as sharply resonant acoustic transducer to detect sound signal instead of conventional wideband-microphone [38–43]. In 2011, Yi et al. [32] used a 7-mw blue laser diode for the first time to demonstrate a trace NO_2 detection in the laboratory using the QEPAS technique. The detection sensitivity and the stability time are not sufficient for ambient NO_2 detection. In order to take advantage of the linear relationship between sensitivity and power, a high power light source is needed, but usually is characterized by a degraded beam quality. This brings a great

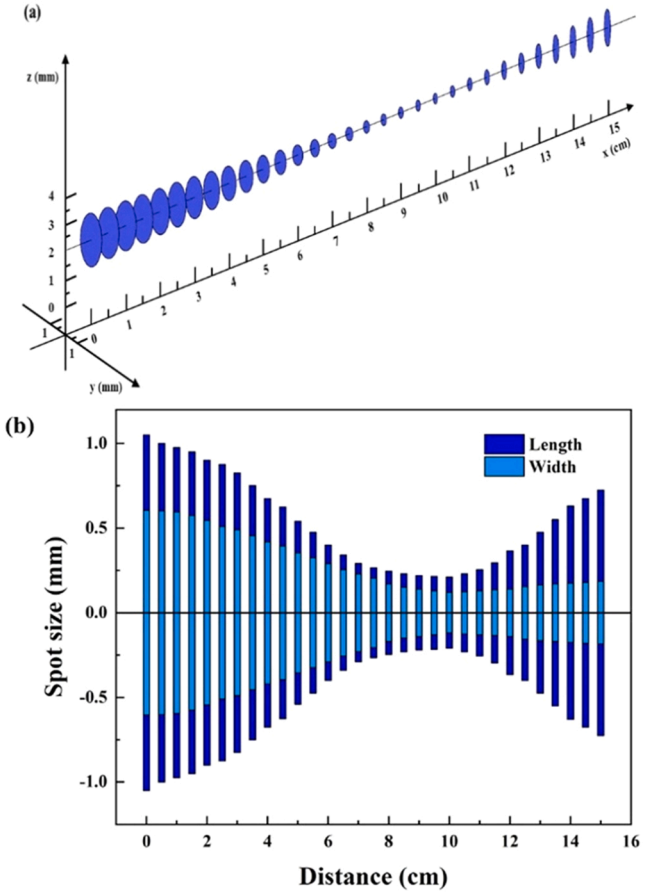

Fig. 4. (a) Schematic diagram of the beam propagation with the lens position as the zero point of the abscissa axis. The spot centers are fixed at the same height. (b) Specific spot size at different distances from the convex lens. The length and width of the laser spot are depicted in dark blue and light blue.

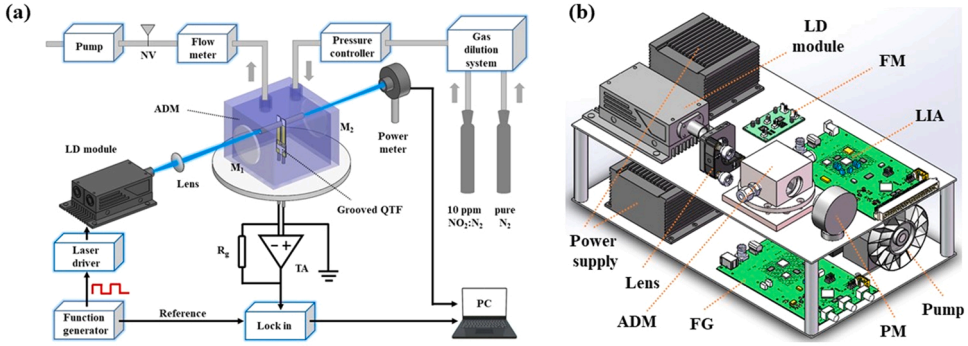

Fig. 3. (a) Schematic of the QEPAS-based NO_2 sensor system combining a grooved QTF and a high-power blue LD module. M_1, M_2: quartz windows; ADM: acoustic detection module; TA: trans-impedance pre-amplifier; FG: function generator; LIA: lock in amplifier; PM: power meter and FM: flow meter. (b) CAD image of the NO_2 sensor with dimensions of length (38 cm), width (23 cm), and height (20 cm).

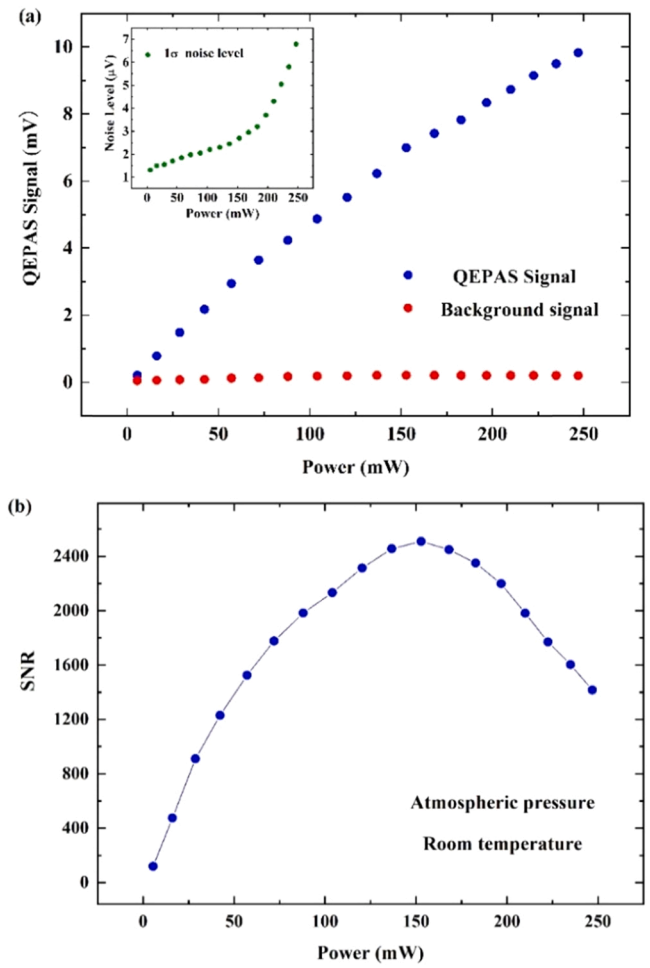

Fig. 5. (a) QEPAS signal as a function of the LD optical power. (b) The signal-to-noise ratio as a function of the LD optical power. Data were obtained with a 10-ppm NO_2:N_2 mixture.

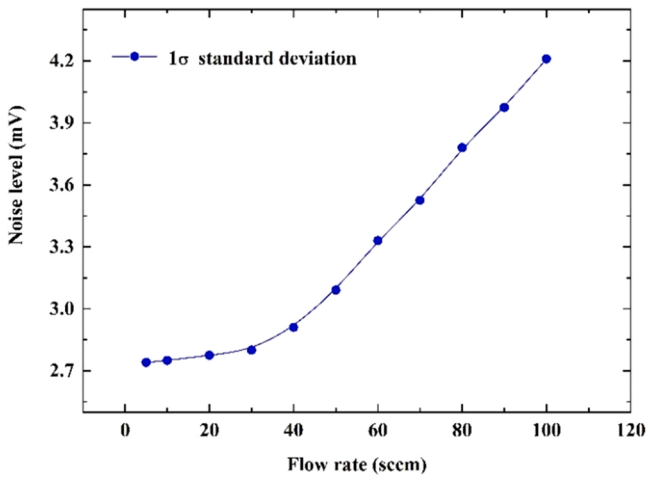

Fig. 6. Dependence of the noise level measured for pure N_2 as a function of the gas flow rate in the range of 5–100 sccm.

challenge to couple a high-power beam through a 300-μm prong-spacing QTF since any light hitting the QTF can cause a large background signal. In 2015, Zheng et al. [44] developed a NO_2 sensor based on the QEPAS technique by use of a 160-mW wide-stripe LED. An electrical modulation cancellation method (E-MOCAM) was demonstrated capable to reduce

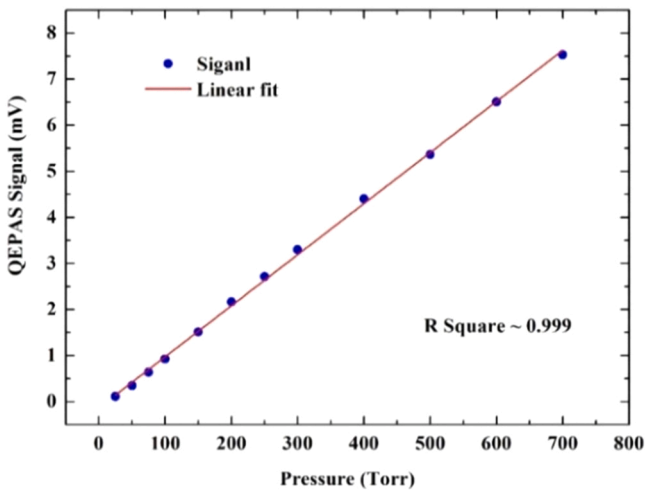

Fig. 7. QEPAS signal as a function of the gas pressure in the ADM from 25 Torr to 700 Torr.

the excessive background signal and a detection limit of 1.3 ppb was obtained at 1-s integration time. But this method increase the complexity of the sensing system and hence reduced its robustness. Moreover, the stability time of the system is only tens of seconds so that a routine calibration must be performed at fixed intervals. In 2016, a scattered light modulation cancellation method (SL-MOCAM) was combined with QEPAS technique to detect the NO_2 and a 1σ detection limit of ~ 60 ppb was achieved at 1-s integration time [45]. This method suppressed background signal by exploiting two light sources: excitation and balance light sources, and extended the stability time up to 360 s. But the issue regarding sensor size was still not solved and this detection sensitivity was insufficient for ambient NO_2 detection. Therefore, the current QEPAS-based sensors can not be employed for long-term ambient NO_2 monitoring, due to the insufficient detection sensitivity or/and the short stability time.

In fact, the MOCAM methods introduce an inverted external signal to balance, rather than eliminate, the background signal which changes slowly over time and external environment. As a result, a passive constant compensation cannot balance the slow drift and hence a long stability time cannot be achieved. To essentially remove this background signal, there are two ways: (1) design and use large-prong-spacing QTF so that the beam can clearly pass through the prong gap of the QTF; (2) employ a light source with an improved beam quality. These two ways should work together to achieve the best results.

In this work, we demonstrate a miniaturized and integrated QEPAS-based NO_2 sensor, in which a custom surface-grooved QTF and a high-power small-sized laser diode (LD) module are used. The grooved QTF has a prong spacing of 0.8 mm and a high quality factor of ~ 15,000, avoiding the use of complicated MOCAM and/or spatial beam filter, and thus reducing the background signal as well as extending the stability time of the sensor. Besides, both prong surfaces have rectangular grooves to enhance the piezoelectric effect of the QTF. By means of the linear relationship between sensitivity and power, the performance of the QEPAS sensor in terms of detection sensitivity and long term stability is significantly improved.

2. Sensor design and characterization

2.1. Selection of the exciting diode laser

According to the HITRAN database [46] , the NO_2 has a broadband absorption from 250 nm to 650 nm and the corresponding absorption cross sections is exhibited in Fig. 1. The absorption cross section of NO_2 gas is large within the wavelength range of 400–450 nm, and a

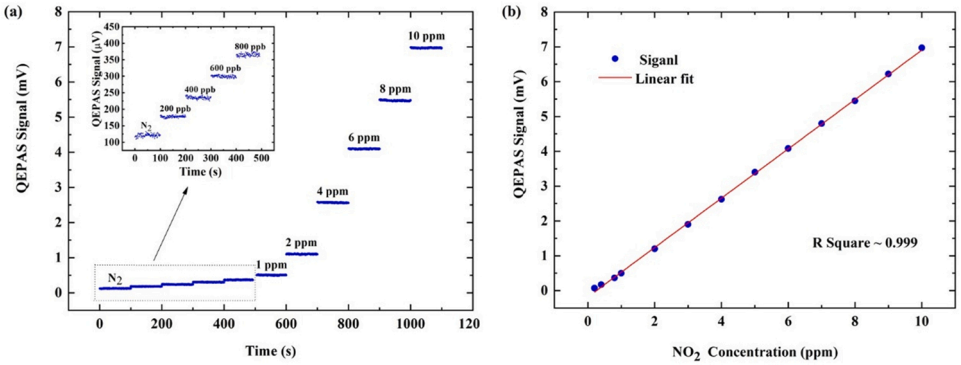

Fig. 8. (a) QEPAS signals recorded as a function of time at different NO_2 concentration levels. (b) Same data averaged and plotted as a function of NO_2 concentration. The red line represents the linearity of the sensor response.

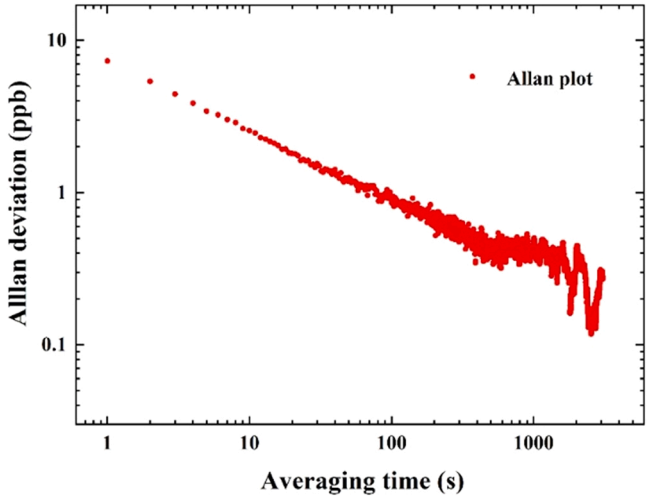

Fig. 9. Allan deviation analysis from time series measurements in pure N_2 for the QEPAS-based sensor system.

maximum cross-section of 7.4×10^{-19} cm^2/molecular is observed at 414 nm. Nevertheless, the wavelength of 414 nm is not the best choice for NO_2 photoacoustic detection due to the photochemical dissociation which can be induced by the excitation laser with $\lambda < 415$ nm as following [1]:

$$NO_2 + h\nu(\lambda < 415\ \text{nm}) \rightarrow NO_2^* \rightarrow NO + O \quad (1)$$

$$O_2 + O + M \rightarrow O_3 + M \quad (2)$$

where NO_2^* represents the NO_2 molecule in the excited state and M represents one of N_2, O_2 and other molecules. Hence the wavelength of the excitation light source should satisfy the condition $\lambda > 415$ nm to avoid the attenuation of photoacoustic signal due to the photolysis.

Considering the excitation wavelength and miniaturization of the laser source, a custom blue multimode LD module (Changchun New Industries Optoelectronics Technology, China) emitting at 450 nm was selected as excitation source of the NO_2-QEPAS sensor with a maximum continuous wave (CW) output power of 3.5 W. The LD module operated at room temperature with a power fluctuations (rms, 24 h) of 3%. The LD emission spectrum was measured by employing a spectrometer (Avantes, Netherland, Model AVS-DESKTOP-USB2) and a spectra width (full width at half maximum) of ~ 7 nm was obtained as shown in Fig. 1. The LD has a beam divergence (full angle) of 1.4×0.2 mrad, bringing significant improvement in the beam quality compared with the Refs. [44,45].

Furthermore, small size is a noticeable feature of this LD module which has an outside dimension of ~ 800 cm^3 ($163 \times 77 \times 65$ mm^3), allowing the laser source to apply to compact gas sensors. In this work, the laser intensity was modulated by a square-wave signal with a duty cycle of 50%, making the average optical power only half that in CW mode. The relationship between the LD average power and the driving voltage was plotted in Fig. 2, showing a good linearity.

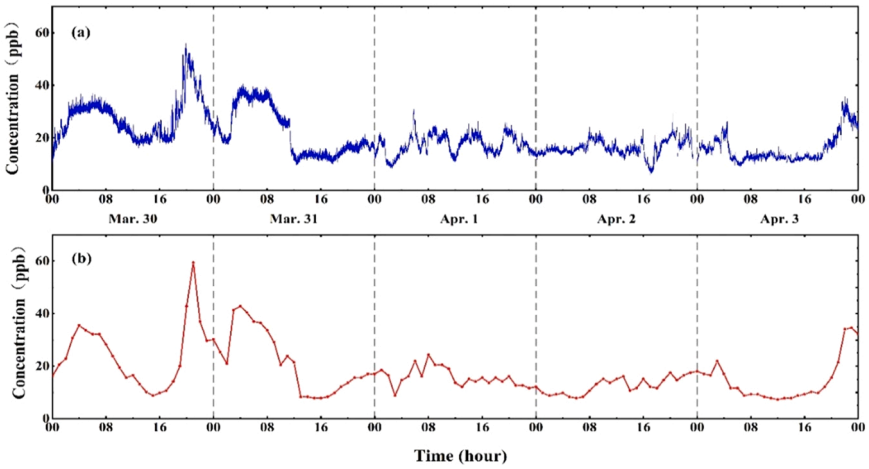

Fig. 10. On-line NO_2 monitoring on the campus of Shanxi University from Mar. 30, 2021 to Apr. 3, 2021 (blue). And the corresponding data available from a nearby station of the CNEMC (red).

Table 1
Intercomparison of four kinds of NO_2 QEPAS Sensor.

Detection technique	Power (mW)	QTF gap (μm)	Stability time (s)	Detection sensitivity (ppb)	Long term on-line monitoring	Refs.
BB-OB-QEPAS	7	300	20	18	No	[27]
E-MOCAM	156	300	1	1.3	No	[38]
SL-MOCAM	4.8	300	360	60	No	[39]
This paper	153	800	590	7.3	Yes	–

2.2. Integrated QEPAS-based NO2 sensor design

The experimental layout of the developed NO_2 sensor based on the high-power blue LD module and the surface-grooved QTF is schematically depicted in Fig. 3. To miniaturize the QEPAS-based system, all the components were integrated into a two-floor architecture which has an outside dimension of 38 × 23 × 20 cm^3. The small-sized blue LD module was used as excitation source to excite QEPAS signal. A laser driver board was employed to control the current and temperature of the LD module. A square-wave signal with a frequency of f_0 from a function generator was applied to the LD by means of the intensity modulation photoacoustic detection approach. Then the modulated laser beam pass through an acoustic detection module (ADM) which consists of a spectrophone and a gas enclosure. Due to the high transmissivity efficiency (95%) at 450 nm, two quartz windows (M_1, M_2) with diameters of 25.4 mm was mounted on the either side of the gas enclosure for optical access. The spectrophone was composed of a custom grooved QTF and two AmRs which symmetrically positioned on both sides of the QTF. The current signal generated from piezoelectric effect of the QTF was amplified by a low noise trans-impedance pre-amplifier (TA) with a feedback resistor R_g of 10 MΩ and then directed to a lock-in amplifier (LIA) board (FEMTO Inc., Germany, Model LIA-BVD-150-H) for demodulation processing. The filter slope and the time constant of the LIA board were set to a 12 dB/oct and 300 ms, respectively, leading to a detection bandwidth Δf of 0.833 Hz. A power meter (PM) was placed behind the ADM to measure the laser power and facilitated the beam alignment. Besides, a gas inlet and outlet were located at the top of the ADM for gas exchange. The gas dilution system (Environics Inc., USA, Model EN4000) diluted a certificated 10-ppm NO_2:N_2 mixture gas with a pure N_2 to produce the NO_2:N_2 mixture gases with different concentration levels for assessing the performance of the NO_2 sensor system. A pressure control module (CFsensor Inc., China, Model XGZP6847A) was combined with a diaphragm pump to control the gas pressure in the ADM. The gas flow rate was adjusted and monitored via a needle valve and a mass flow sensor (Consensic Inc., Model CAFS3000), respectively.

The custom-made QTF used in the spectrophone is a grooved QTF with a resonance frequency of 15.2 kHz which was acoustically coupled with two identical AmRs with an inner diameter of 1.65 mm and a length of 7 mm, forming an on-beam QEPAS configuration. A signal enhancement factor of ~ 30 is achieved with such an optimum configuration compared to the bare grooved QTF without AmRs. The two prongs of the grooved QTF are separated by 800 μm, and the QTF has a prong length l of 9.4 mm, a width w of 2 mm, and a thickness t of 0.25 mm. Furthermore, four rectangular grooves with an area of 1.8 × 7 mm^2 and depth of 0.05 mm were carved on each QTF prong surface in order to provide a reduced electrical resistance R without affecting the quality factor Q. Such a modified QTF has a R value of 107.15 kΩ and Q-factor of 15022, effectively enhancing the piezoelectric effect of the QTF. The details of the QTF design are described in Refs. [47–49]. The QEPAS signal amplitude S can be expressed as [50–52]:

$$S \propto \alpha P Q / f_0 \tag{3}$$

where α is the absorption coefficient, P is the laser power, Q and f_0 is the quality factor and the resonance frequency of QTF. The custom grooved QTF having a resonance frequency of 15.2 kHz can provide a higher QEPAS signal than a 32.7-kHz standard QTF under the same condition, according to Eq. (3).

The employed LD is a multimode laser source which has an elliptical beam spot with a divergence of 1.4 × 0.2 mrad. Hence a convex quartz lens with 100-mm focal length was utilized to focus the elliptical beam so that it can pass through the spectrophone. As shown in Fig. 4(a), the beam propagation through the ADM was detected by a Pyrocam IIIHR Beam Profiling Camera, demonstrating the dimensional change of laser spot along beam propagation path. The detailed size parameters of the laser spot at different distances from the convex lens are depicted in Fig. 4(b) and all measurements were operated at the same height which is defined as the zero point of the y-axis. The minimum lengths of major and minor axis of the elliptical laser spots are 840 μm and 500 μm, respectively, at the focal point of the lens (x = 10 cm), demonstrating that the converging laser beam can pass through the prong spacing (800 μm) of the grooved QTF without being blocked.

3. Results and discussion

3.1. Parameter optimization of sensor system

Based on Eq. (3), the QEPAS signal is proportional to the incident optical power since more gas molecules are excited to higher energy levels with power increasing, thereby the NO_2 sensor performance can benefit from the high laser power. However, the background signal and noise level induced by the stray light due to the multimode nature of the LD also increase with the laser power rising. Here the background signal refers to the offset of the zero baseline of QEPAS signal, while the noise level is defined as the random disturbance of QEPAS signal when measuring a specific gas concentration. In this work, a certified 10-ppm N_2:NO_2 gas mixture (Nanjing Special Gas Factory Co., Ltd.) was flushed into the ADM at atmospheric pressure and the gas flow rate was set to 30 sccm (standard-state cubic centimeter per minute). The relationship between QEPAS signal, noise and laser power was investigated as shown in Fig. 5(a). No significant variations in the background signal are observed with the power increasing, while the 1σ noise level significantly increases when the laser power is > 160 mW, as shown in the inset. The signal-noise-ratio (SNR) which is an important performance parameter of sensors are plotted in Fig. 5(b) according to the following equation:

$$\mathrm{SNR} = \frac{S_{QEPAS} - S_{BS}}{S_n} \tag{4}$$

where S_{QEPAS}, S_{BS}, S_n are the QEPAS signal amplitude, the background signal and the 1σ noise level, respectively. As described in Fig. 5(b), the SNR value increases gradually with the laser power increasing until a maximum is reached and then decreases. The maximum QEPAS SNR of 2510 was achieved at laser power of 153 mW. The corresponding driving voltage of the LD module is 2 V according to Fig. 3 and hence this optimum voltage value was selected in the following experiments.

When the inner volume of the ADM is defined, a faster response time can be achieved with a faster gas flow rate. However, the noise level grows with the gas flow rate since the gas turbulence disturbs the QTF prongs. The 1σ noise level is depicted in Fig. 6 as a function of the nitrogen flow rate ranging from 5 sccm to 100 sccm. The results show that the 1σ noise value increases by only 6% when the gas flow rate increases from 5 sccm to 40 sccm, while a rapid increase of the noise level occurs when the gas flow rate is > 50 sccm. Thus 40 sccm was selected as the optimum flow rate for the QEPAS-based NO_2 sensor operation. A gas

exchange time of 110 s was experimentally measured for the 70-cm^3 inner volume of the ADM.

In QEPAS, the pressure in ADM has to be taken into account since the quality factor of QTF, the vibration-translation relaxation and the intensity of absorption spectrum are all pressure dependent. Therefore, the gas pressure must be optimized and chosen appropriately for the optimization of the sensor performance. Fig. 7 shows the relationship between the QEPAS signal and the gas pressure from 25 Torr to 700 Torr. Although the *Q*-factor of the QTF decreases as the pressure increases, the intensity of the absorption spectrum and the V-T relaxation rate of gas molecules increases when the gas pressure rises. Therefore, a linear relationship (R Square ~ 0.999) between the gas pressure and the QEPAS signal is observed. Hence the atmospheric pressure was determined as the optimum operating pressure and thus there was no need for the sensor pressure control, further simplifying the NO_2 sensor.

3.2. Sensor performance assessment

In order to assess the sensor performance for the NO_2 detection, the QEPAS response to the NO_2:N_2 mixtures in the concentration range of 0–10 ppm were measured and analyzed as shown in Fig. 8(a). These data were acquired at 1-s acquisition time under atmospheric pressure and the parameters (the laser power, the flow rate and the gas pressure) were fixed at the optimum values. The inset shows that a background signal of 120 μV was obtained when pure N_2 was fed into the ADM. The QEPAS signals under different NO_2 concentration were averaged, as shown in Fig. 8(b). The linear relationship with *R* square of 0.999 confirms the linearity of the NO_2 sensor response to concentration level. With 200-ppb NO_2:N_2 mixture flushed into the system, a minimum detection limit (MDL) of 7.3 ppb with 0.833-Hz detection bandwidth (300-ms time constant and 12-dB filter slope) was achieved which is ~ 8 times lower than the SL-MOCAM based QEPAS sensor reported previously [45]. Due to the LD module which was used to probe a broadband absorption feature, the average cross-section of the LD emission spectrum must be weighted from 448 nm to 452 nm, resulting in an effective absorption cross-section of 4.67×10^{-19} cm^2/molecular. Hence the normalized noise equivalent absorption (NNEA) coefficient was calculated to be 1.54×10^{-8} cm^{-1} $W/Hz^{1/2}$.

In addition, the optimum achievable sensitivity and long-term drifts of the NO_2 sensor system was investigated by performing an Allan deviation analysis which is shown in Fig. 9. The Allan analysis predicts the trend of the MDL value as a function of the averaging time by measuring and averaging the QEPAS signal in pure N_2. With the optimum averaging time of 590 s, the corresponding detection sensitivity of 0.31 ppb can be extracted which means that white noise remains the dominant noise source for 590 s, demonstrating the excellent stability and reliability of the developed QEPAS-based sensor.

To test the ability of on-line real-time monitoring of the grooved-QTF-based QEPAS sensor, a continuous five-day monitoring of ambient NO_2 outside a laboratory, located in the Shaw Amenities Building on the Shanxi University campus in China, with GPS coordinates: 37°47′58.1″N 112°35′14.2″E, was carried out and the obtained results are shown in Fig. 10. The sensor system was placed indoors and the atmospheric air was pumped into the ADM by a diaphragm pump. This measurement was carried out at atmospheric pressure with an acquisition time of 1 s. In order to filter dust and particulate matter, a micropore membrane with a diameter of 3 μm made of PTFE was inserted at the air inlet of the Teflon tube.

The NO_2 concentration was measured over the period of Mar. 30, 2021–Apr. 3, 2021. The results were compared with the NO_2 concentration data published by China National Environmental Monitoring Center (CNEMC) [53] and the excellent consistency verifies the accuracy and validity of the NO_2 sensor system. Since the CNEMC employs a chemiluminescence detection system, suffering from a limited data updating rate of 1 data point/hour, which implies all data during every hour was averaged, some details of the concentration variations may be lost. Furthermore, the distance between two sensor systems is 7 km. The local meteorological conditions, such as wind, and traffic conditions were different, which can cause the small inconsistence of the measured results. For example, concentration peaks occurred at 16:00 on Mar. 30, 2021 and 17:14 on Apr. 2, 2021 shown in Fig. 10 (a), but the counterparts were not observed in Fig. 10 (b).

4. Conclusions

In conventional photodetector-based laser gas sensing, there is no way to employ a high-power laser source to improve the detection sensitivity of a sensor, due to the fact that the upper limit of the excitation optical power is usually subject to the saturation power of the photodetector. Nevertheless, in photoacoustic spectroscopy, sound waves rather than light waves are detected. The dynamic range of a sound transducer for sound detecting can be up to 130 dB and especially a QTF in QEPAS can ensure a linear response over four orders of magnitude. In this work, we demonstrated the realization of a compact QEPAS sensor for ppb-level ambient NO_2 detection, exploiting the linearity between QEPAS singal and laser power. A minimum detectable concentration (1σ) of 7.3 ppb at the averaging time of 1 s and the stability time of 590 s were achieved with an excitation optical power of ~ 150 mW, which is very suitable for continuous ambient monitoring. Although there is a linear relationship between sensitivity and power in QEPAS, how much optical power can be used depends on the coupling quality of the QTF and the laser beam. A poor coupling quality will cause large background signal and noise level in the case of a high power excitation. Hence, when the QTF geometry and the beam quality are determined, there is an optimal excitation optical power maximizing the SNR. Thanks to the new QTF design and the custom LD module, the reported sensor exploits as much optical power as possible to improve the detection sensitivity without degrading stability time. Compared with MOCAM, the reported sensor provided a smaller size, a higher detection sensitivity and a longer stability time. The side-by-side comparison between the QEPAS-based NO_2 sensors demonstrated so far is listed in Table 1. The results show that the reported sensor provides the best performance. Deployment of the sensor system in a vehicle operation test to assess its performance for ambient NO_2 monitoring will be conducted in the future.

Declaration of Competing Interest

The authors declare that there are no conflicts of interest.

Acknowledgement

The project is sponsored by National Key R&D Program of China (No. 2019YFE0118200); National Natural Science Foundation of China (NSFC) (Nos. 62075119, 62175137, 61805132, 62122045); THORLABS GmbH, within PolySense, a joint-research laboratory; Sanjin Scholar (No. 2017QNSJXZ-04); Shanxi "1331KSC", and Scientific and Technological Innovation Programs of Higher Education Institutions in Shanxi (2019L0028).

References

[1] J.H. Seinfeld, S.N. Pandis, Atmospheric Chemistry and Physics: From Air Pollution to Climate Change, John Wiley & Sons, New York, 1998.
[2] A.P. Vasilkov, J. Joiner, L. Oreopoulos, J.F. Gleason, P. Veefkind, E. Bucsela, E. A. Celarier, R.J.D. Spurr, S. Platnick, Impact of tropospheric nitrogen dioxide on the regional radiation budget, Atmos. Chem. Phys. 9 (17) (2009) 6389–6400.
[3] S. Solomon, W. Portmann, R.W. Sanders, J.S. Daniel, W. Madsen, B. Bartram, E. G. Dutton, On the role of nitrogen dioxide in the absorption of solar radiation, J. Geophys. Res 104 (D10) (1999) 12047–12058.
[4] J. Beauchamp, A. Wisthaler, W. Grabmer, C. Neuner, A. Weber, A. Hansel, Short-term measurements of CO, NO, NO_2, organic compounds and PM10 at a motorway location in an Austrian valley, Atmos. Environ. 38 (16) (2004) 2511–2522.
[5] D.C. Carslaw, S.D. Beevers, Investigating the potential importance of primary NO_2 emissions in a street canyon, Atmos. Environ. 38 (22) (2004) 3585–3594.

[6] D.C. Carslaw, S.D. Beevers, Estimations of road vehicel primary NO_2 exhaust emission fractions using monitoring data in London, Atmos. Environ. 39 (1) (2005) 167–177.
[7] E.J. Dunlea1, S.C. Herndon, D.D. Nelson, R.M. Volkamer1, F.S. Martini, P. M. Sheehy, M.S. Zahniser, J.H. Shorter, J.C. Wormhoudt, B.K. Lamb, E.J. Allwine, J.S. Gaffney, N.A. Marley, M. Grutter, C. Marquez, S. Blanco, B. Cardenas, A. Retama, C.R. Ramos Villegas, C.E. Kolb, L.T. Molina, M.J. Molina, Evaluation of nitrogen dioxide chemiluminescence monitors in a polluted urban environment, Atmos. Chem. Phys. 7 (1) (2007) 569–604.
[8] T. Wu, W. Zhao, W. Chen, W. Zhang, X. Gao, Incoherent broadband cavity enhanced absorption spectroscopy for in situ measurements of NO_2 with a blue light emitting diode, Appl. Phys. B: Lasers Opt. 94 (1) (2009) 85–94.
[9] G. Villena, I. Bejan, R. Kurtenbach, P. Wiesen, J. Kleffmann, Development of a new long path absorption photometer (LOPAP) instrument for the sensitive detection of NO_2 in the atmosphere, Atmos. Meas. Tech. 4 (8) (2011) 1663–1676.
[10] P.L. Kebabian, S.C. Herndon, A. Freedman, Detection of nitrogen dioxide by cavity attenuated phase shift spectroscopy, Anal. Chem. 77 (2) (2005) 724–728.
[11] Y. Matsumi, F. Taketani, K. Takahashi, T. Nakayama, M. Kawai, Y. Miyao, Fluorescence detection of atmospheric nitrogen dioxide using a blue light-emitting diode as an excitation source, Appl. Opt. 49 (19) (2010) 3762–3767.
[12] A. Richter, J.P. Burrows, H. Nüß, C. Granier, U. Niemeier, Increase in tropospheric nitrogen dioxide over China observed from space, Nature 437 (7055) (2005) 129–132.
[13] Y. Matsumi, S. Murakami, M. Kono, K. Takahashi, M. Koike, Y. Kondo, High sensitivity instrument for measuring atmospheric NO_2, Anal. Chem. 73 (22) (2001) 5485–5493.
[14] W. Ren, W.Z. Jiang, F.K. Tittel, Single-QCL-based absorption sensor for simultaneous trace-gas detection of CH_4 and N_2O, Appl. Phys. B 117 (1) (2014) 245–251.
[15] I.B. Pollack, B.M. Lerner, T.B. Ryerson, Evaluation of ultraviolet light-emitting diodes for detection of atmospheric NO_2 by photolysis-chemiluminescence, J. Atmos. Chem. 65 (2–3) (2010) 111–125.
[16] J. Peltola, T. Hieta, M. Vainio, Parts-per-trillion-level detection of nitrogen dioxide by cantilever-enhanced photo-acoustic spectroscopy, Opt. Lett. 40 (13) (2015) 2933–2936.
[17] R.M. Garnica, M.F. Appel, L. Eagan, J.R. McKeachie, T. Benter, A. REMPI, method for the ultrasensitive detection of NO and NO_2 using atmospheric pressure laser ionization mass spectrometry, Anal. Chem. 72 (22) (2000) 5639–5646.
[18] Y.Q. Li, K.L. Demerjian, M.S. Zahniser, D.D. Nelson, J.B. McManus, S.C. Herndon, Measurement of formaldehyde, nitrogen dioxide, and sulfur dioxide at Whiteface Mountain using a dual tunable diode laser system, J. Geophys. Res.: Atmos. 109 (D16) (2004).
[19] S. Qiao, Y. Ma, Y. He, P. Patimisco, A. Sampaolo, V. Spagnolo, Ppt level carbon monoxide detection based on light-induced thermoelastic spectroscopy exploring custom quartz tuning forks and a mid-infrared QCL, Opt. Express 29 (16) (2021) 25100–25108.
[20] S. Qiao, Y. He, Y. Ma, Trace gas sensing based on single-quartz-enhanced photoacoustic–photothermal dual spectroscopy, Opt. Lett. 46 (10) (2021) 2449–2452.
[21] Z. Lang, S. Qiao, Y. He, Y. Ma, Quartz tuning fork-based demodulation of an acoustic signal induced by photo-thermo-elastic energy conversion, Photoacoustics 22 (2021), 100272.
[22] Y. Ma, R. Lewicki, M. Razeghi, F.K. Tittel, QEPAS based ppb-level detection of CO and N_2O using a high power CW DFB-QCL, Opt. Express 21 (1) (2013) 1008–1019.
[23] X. Yin, M. Gao, R. Miao, L. Zhang, X. Zhang, L. Liu, X. Shao, F.K. Tittel, Near-infrared laser photoacoustic gas sensor for simultaneous detection of CO and H_2S, Opt. Express 29 (21) (2021) 34258–34268.
[24] J. Harder, E. Williams, K. Baumann, F. Fehsenfeld, Ground-based comparison of NO_2, H_2O, and O_3 measured by long-path and in situ techniques during the 1993 Tropospheric OH Photochemistry Experiment, J. Geophys. Res. 102 (D5) (1997) 6227–6243.
[25] J.A. Thornton, P.J. Wooldridge, R.C. Cohen, Atmospheric NO_2: in situ laser-induced fluorescence detection at parts per trillion mixing ratios, Anal. Chem. 72 (3) (2000) 528–539.
[26] P. Ehlers, I. Silander, J. Wang, A. Foltynowicz, O. Axner, Fiber-laser-based noise-immune cavity-enhanced optical heterodyne molecular spectrometry incorporating an optical circulator, Opt. Lett. 39 (2) (2014) 279–282.
[27] Z. Li, W. Ma, X. Fu, W. Tan, G. Zhao, L. Dong, L. Zhang, W. Yin, S. Jia, Continuous-wave cavity ringdown spectroscopy based on the control of cavity reflection, Opt. Express 21 (15) (2013) 17961–17971.
[28] H. Fuchs, W.P. Dubé, B.M. Lerner, N.L. Wagner, E.J. Williams, S.S. Brown, A sensitive and versatile detector for atmospheric NO_2 and NO_x based on blue diode laser cavity ring-down spectroscopy, Environ. Sci. Technol. 43 (20) (2009) 7831–7836.
[29] R. Wada, A.J. Orr-Ewing, Continuous wave cavity ring-down spectroscopy measurement of NO_2 mixing ratios in ambient air, Analyst 130 (12) (2005) 1595–1600.
[30] X. Yin, L. Dong, H. Wu, H. Zheng, W. Ma, L. Zhang, W. Yin, S. Jia, F.K. Tittel, Sub-ppb nitrogen dioxide detection with a large linear dynamic range by use of a differential photoacoustic cell and a 3.5 W blue multimode diode laser, Sens. Actuators B Chem. 247 (2017) 329–335.
[31] Y. Pan, L. Dong, X. Yin, H. Wu, Compact and highly sensitive NO_2 photoacoustic sensor for environmental monitoring, Molecules 25 (5) (2020) 1201.
[32] H. Yi, K. Liu, W. Chen, T. Tan, L. Wang, X. Gao, Application of a broadband blue laser diode to trace NO_2 detection using off-beam quartz enhanced photoacoustic spectroscopy, Opt. Lett. 36 (4) (2011) 481–483.
[33] T. Wei, A. Zifarelli, S.D. Russo, H. Wu, G. Menduni, P. Patimisco, A. Sampaolo, V. Spagnolo, L. Dong, High and flat spectral responsivity of quartz tuning fork used as infrared photodetector in tunable diode laser spectroscopy, Appl. Phys. Rev. 8 (2021), 041409.
[34] H. Zheng, Y. Liu, H. Lin, B. Liu, X. Gu, D. Li, B. Huang, Y. Wu, L. Dong, W. Zhu, J. Tang, H. Guan, H. Lu, Y. Zhong, J. Fang, Y. Luo, J. Zhang, J. Yu, Z. Chen, F. K. Tittel, Quartz-enhanced photoacoustic spectroscopy employing pilot line manufactured custom tuning forks, Photoacoustics 17 (2020), 100158.
[35] M. Pushkarsky, A. Tsekoun, I.G. Dunayevskiy, R. Go, C.K.N. Patel, Sub-parts-per-billion level detection of NO_2 using room-temperature quantum cascade lasers, Proc. Natl. Acad. Sci. USA 103 (29) (2006) 10846–10849.
[36] A.A. Kosterev, F.K. Tittel, D.V. Serebryakov, A.L. Malinovsky, I.V. Morozov, Applications of quartz tuning forks in spectroscopic gas sensing, Rev. Sci. Instrum. 76 (4) (2005), 043105.
[37] A.A. Kosterev, Y.A. Bakhirkin, R.F. Curl, F.K. Tittel, Quartz-enhanced photoacoustic spectroscopy, Opt. Lett. 27 (21) (2002) 1902–1904.
[38] L. Dong, A.A. Kosterev, D. Thomazy, F.K. Tittel, QEPAS spectrophones: design, optimization, and performance, Appl. Phys. B: Lasers Opt. 100 (3) (2010) 627–635.
[39] P. Patimisco, A. Sampaolo, L. Dong, F.K. Tittel, V. Spagnolo, Recent advances in quartz enhanced photoacoustic sensing, Appl. Phys. Rev. 5 (1) (2018), 011106.
[40] H. Wu, L. Dong, H. Zheng, Y. Yu, W. Ma, L. Zhang, W. Yin, L. Xiao, S. Jia, F. K. Tittel, Beat frequency quartz-enhanced photoacoustic spectroscopy for fast and calibration-free continuous trace-gas monitoring, Nat. Commun. 8 (1) (2017) 15331.
[41] L. Hu, C. Zheng, M. Zhang, K. Zheng, J. Zheng, Z. Song, X. Li, Y. Zhang, Y. Wang, F. K. Tittel, Long-distance in-situ methane detection using near-infrared light-induced thermo-elastic spectroscopy, Photoacoustics 21 (2021), 100230.
[42] K. Liu, X. Guo, H. Yi, W. Chen, W. Zhang, X. Gao, Off-beam quartz-enhanced photoacoustic spectroscopy, Opt. Lett. 34 (10) (2009) 1594–1596.
[43] X. Yin, H. Wu, L. Dong, B. Li, W. Ma, L. Zhang, W. Yin, L. Xiao, S. Jia, F.K. Tittel, Ppb-level SO_2 photoacoustic sensors with a suppressed absorption-desorption effect by using a 7.41 μm external-cavity quantum cascade laser, Acs Sens. 5 (2020) 549–556.
[44] H. Zheng, L. Dong, X. Yin, X. Liu, H. Wu, L. Zhang, W. Ma, W. Yin, S. Jia, Ppb-level QEPAS NO_2 sensor by use of electrical modulation cancellation method with a high power blue LED, Sens. Actuators B Chem. 208 (2015) 173–179.
[45] H. Zheng, L. Dong, Y. Ma, H. Wu, X. Liu, X. Yin, L. Zhang, W. Ma, W. Yin, L. Xiao, S. Jia, Scattered light modulation cancellation method for sub-ppb-level NO_2 detection in a LD-excited QEPAS system, Opt. Express 24 (10) (2016) A752–A761.
[46] The HITRAN Database: ⟨http://www.hitran.com⟩.
[47] P. Patimisco, A. Sampaolo, M. Giglio, S.D. Russo, V. Mackowiak, H. Rossmadl, A. Cable, F.K. Tittel, V. Spagnolo, Tuning forks with optimized geometries for quartz-enhanced photoacoustic spectroscopy, Opt. Express 27 (2) (2019) 1401–1415.
[48] P. Patimisco, A. Sampaolo, L. Dong, M. Giglio, G. Scamarcio, F.K. Tittel, V. Spagnolo, Analysis of the electro-elastic properties of custom quartz tuning forks for optoacoustic gas sensing, Sens. Actuators B Chem. 227 (2016) 539–546.
[49] S. Li, L. Dong, H. Wu, A. Sampaolo, P. Patimisco, V. Spagnolo, F.K. Tittel, Ppb-level quartz-enhanced photoacoustic detection of carbon monoxide exploiting a surface grooved tuning fork, Anal. Chem. 91 (9) (2019) 5834–5840.
[50] H. Wu, L. Dong, H. Zheng, X. Liu, X. Yin, W. Ma, L. Zhang, W. Yin, S. Jia, F.K. Tittel, Enhanced near-infrared QEPAS sensor for sub-ppm level H_2S detection by means of a fiber amplified 1582 nm DFB laser, Sens. Actuators B Chem. 221 (2015) 666–672.
[51] H. Wu, L. Dong, X. Yin, A. Sampaolo, P. Patimisco, W. Ma, L. Zhang, W. Yin, L. Xiao, V. Spagnolo, S. Jia, Atmospheric CH_4 measurement near a landfill using an ICL-based QEPAS sensor with V-T relaxation self-calibration, Sens. Actuators B Chem. 297 (2019), 126753.
[52] H. Wu, A. Sampaolo, L. Dong, P. Patimisco, X. Liu, H. Zheng, X. Yin, W. Ma, L. Zhang, W. Yin, V. Spagnolo, S. Jia, F.K. Tittel, Quartz enhanced photoacoustic H_2S gas sensor based on a fiber-amplifier source and a custom tuning fork with large prong spacing, Appl. Phys. Lett. 107 (2015), 111104.
[53] China National Environmental Monitoring Center. ⟨http://www.cnemc.cn/⟩.

Shangzhi Li is now pursuing a Ph.D. degree in atomic and molecular physics in the Institute of Laser Spectroscopy of Shanxi University, China. His research interests include gas sensor, photoacoustic spectroscopy and laser spectroscopy techniques.

Juncheng Lu is now pursuing a master degree in Optical Engineering in the Institute of Information Optics of Zhejiang Normal University, China. His research interests include gas sensor and laser spectroscopy techniques.

Zhijin Shang is now pursuing a Ph.D. degree in atomic and molecular physics in the Institute of Laser Spectroscopy of Shanxi University, China. His research interests include optical sensors and photoacoustic spectroscopy.

Xiangbao Zeng received his master degree in Measuring and Testing Technologies and Instruments from jilin University, China, in 2017. From September, 2019, he Studying for a Ph.D. degree in Chongqing University. Currently he is a senior engineer in the CETC. His research activities research activities are focused on acoustic and optical sensors, and sensors applications in environmental monitoring industrial and process control.

Yupeng Yuan received his Ph.D. degree in control theory and control engineering from Chongqing University, China, in 2016. Currently he is a senior engineer in Chongqing Acoustic-Optic-Electronic Co. Ltd, China Electronics Technology Group, Chongqing, China. His research activities are focused on research and development in intelligent sensor and Micro-Electro-Mechanical Systems applied to gas detection, photoelectric transmission and inertial navigation. He has published more than 30 peer reviewed papers.

Hongpeng Wu received his Ph.D. degree in atomic and molecular physics from Shanxi University, China, in 2017. From 2015 to 2016, he studied as a joint Ph.D. student in the electrical and computer engineering department and rice quantum institute, Rice University, Houston, USA. Currently he is a professor in the Institute of Laser Spectroscopy of Shanxi University. His research interests include optical sensors and laser spectroscopy techniques.

Yufeng Pan received his master's degree in atomic and molecular physics from Shanxi University, China, in 2021. Currently he is a Ph.D. student in optical engineering at Huazhong University of Science and Technology. His research interests include optical sensors and laser spectroscopy techniques.

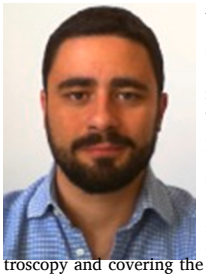

Angelo Sampaolo obtained his Master degree in Physics in 2013 and the Ph.D. Degree in Physics in 2017 from University of Bari. He was an associate researcher in the Laser Science Group at Rice University from 2014 to 2016 and associate researcher at Shanxi University since 2018. Since May 2017, he was a Post-Doctoral Research associate at University of Bari and starting from December 2019, he is Assistant Professor at Polytechnic of Bari. His research activity has included the study of the thermal properties of heterostructured devices via Raman spectroscopy. Most recently, his research interest has focused on the development of innovative techniques in trace gas sensing, based on Quartz-Enhanced Photoacoustic Spectroscopy and covering the full spectral range from near-IR to THz. His achieved results have been acknowledged by a cover paper in Applied Physics Letter of the July 2013 issue.

Pietro Patimisco obtained the Master degree in Physics (cum laude) in 2009 and the Ph.D. Degree in Physics in 2013 from the University of Bari. Since 2018, he is Assistant professor at the Technical University of Bari. He was a visiting scientist in the Laser Science Group at Rice University in 2013 and 2014. Dr. Patimisco's scientific activity addressed both micro-probe optical characterization of semiconductor optoelectronic devices and optoacoustic gas sensors. Recently, his research activities included the study and applications of trace-gas sensors, such as quartz-enhanced photoacoustic spectroscopy and cavity enhanced absorption spectroscopy in the mid infrared and terahertz spectral region, leading to several publications, including a cover paper in Applied Physics Letter of the July 2013 issue.

Vincenzo Spagnolo obtained the Ph.D. in physics in 1994 from University of Bari. From 1997 to 1999, he was researcher of the National Institute of the Physics of Matter. Since 2004, he works at the Technical University of Bari, formerly as assistant and associate professor and, starting from 2018, as full Professor of Physics. Since 2019, he is vice-rector of the Technical University of Bari, deputy to technology transfer. He is the director of the joint-research lab PolySense between Technical University of Bari and THORLABS GmbH, fellow member of SPIE and senior member of OSA. His research interests include optoacoustic gas sensing and spectroscopic techniques for real-time monitoring. His research activity is documented by more than 220 publications and two filed patents. He has given more than 50 invited presentations at international conferences and workshops.

Lei Dong received his Ph.D. degree in optics from Shanxi University, China, in 2007. From June, 2008 to December, 2011, he worked as a post-doctoral fellow in the Electrical and Computer Engineering Department and Rice Quantum Institute, Rice University, Houston, USA. Currently he is a professor in the Institute of Laser Spectroscopy of Shanxi University. His research activities research activities are focused on research and development in laser spectroscopy, in particular photoacoustic spectroscopy applied to sensitive, selective and real-time trace gas detection, and laser applications in environmental monitoring, chemical analysis, industrial process control, and medical diagnostics. He has published more than 100 peer reviewed papers with $>$ 2200 positive citations.